1521-0111/12/8203-361–371
MOLECULAR PHARMACOLOGY
U.S. Government work not protected by U.S. copyright
*Mol Pharmacol* 82:361–371, 2012

Vol. 82, No. 3
79335/3789840



*MINIREVIEW*

# New Insights for Drug Design from the X-Ray Crystallographic Structures of G-Protein-Coupled Receptors

Kenneth A. Jacobson and Stefano Costanzi

*Molecular Recognition Section, Laboratory of Bioorganic Chemistry (K.A.J.), and Laboratory of Biological Modeling (S.C.), National Institutes of Diabetes and Digestive and Kidney Diseases, National Institutes of Health, Bethesda, Maryland*

Received April 16, 2012; accepted June 13, 2012

## ABSTRACT

Methodological advances in X-ray crystallography have made possible the recent solution of X-ray structures of pharmaceutically important G protein-coupled receptors (GPCRs), including receptors for biogenic amines, peptides, a nucleoside, and a sphingolipid. These high-resolution structures have greatly increased our understanding of ligand recognition and receptor activation. Conformational changes associated with activation common to several receptors entail outward movements of the intracellular side of transmembrane helix 6 (TM6) and movements of TM5 toward TM6. Movements associated with specific agonists or receptors have also been described [e.g., extracellular loop (EL) 3 in the $A_{2A}$ adenosine receptor]. The binding sites of different receptors partly overlap but differ significantly in ligand orientation, depth, and breadth of contact areas in TM regions and the involvement of the ELs. A current challenge is how to use this structural information for the rational design of novel potent and selective ligands. For example, new chemotypes were discovered as antagonists of various GPCRs by subjecting chemical libraries to in silico docking in the X-ray structures. The vast majority of GPCR structures and their ligand complexes are still unsolved, and no structures are known outside of family A GPCRs. Molecular modeling, informed by supporting information from site-directed mutagenesis and structure-activity relationships, has been validated as a useful tool to extend structural insights to related GPCRs and to analyze docking of other ligands in already crystallized GPCRs.

## Introduction

In the past 5 years, progress in the structure-based design of ligands for G protein-coupled receptors (GPCRs) has greatly accelerated. The major contributing factor has been the elucidation of X-ray crystallographic structures of high resolution for various drug-relevant GPCRs, initially in the inactive antagonist-bound forms and more recently in agonist-bound forms. The initial breakthrough were the reports in 2007 by the groups of Kobilka (Stanford Univ.), Stevens (Scripps Research Inst.), Schertler and Tate (Medical Research Council Laboratory of Molecular Biology in Cambridge, UK), and colleagues of the first nonrhodopsin GPCR structure (e.g., the inactive human $\beta_2$-adrenergic receptor in complex with the inverse agonist carazolol) (Cherezov et al., 2007; Rasmussen et al., 2007; Rosenbaum et al., 2007). These landmark studies were followed by the determination of other GPCRs (Table 1), and the rapid pace of these reports is continuing. Biogenic amine receptor complexes (epinephrine, dopamine, histamine, muscarinic), nucleoside (adenosine) receptor complexes, sphingolipid ($S1P_1$) receptor complexes, and peptide (CXCR4, opioid) receptor complexes have been reported. All of the crystallized receptors belong to the GPCR family known as class A, family 1, or rhodopsin family, which in humans accounts for more than 80% of all GPCRs

This work was supported by the National Institutes of Health National Institute of Diabetes and Digestive and Kidney Diseases [Grants Z01-DK031126-08, Z01-DK013025-05].

Article, publication date, and citation information can be found at http://molpharm.aspetjournals.org.

http://dx.doi.org/10.1124/mol.112.079335.

**ABBREVIATIONS:** GPCR, G protein-coupled receptor; S1P, sphingosine-1-phosphate; EL, extracellular loop; FAUC50, (*R*)-5-(2-((4-(3-((2-aminoethyl)disulfanyl)propoxy)-3-methoxyphenethyl)amino)-1-hydroxyethyl)-8-hyfroxyquinolin-2(1H)-one; UK-432097, 2-(3-[1-(pyridin-2-yl)piperidin-4-yl]ureido)ethyl-6-*N*-(2,2-diphenylethyl)-5′-*N*-ethylcarboxamidoadenosine-2-carboxamide; ZM241385, 4-(2-(7-amino-2-(furan-2-yl)-[1,2,4]triazolo[1,5-*a*][1,3,5]triazin-5-ylamino)ethyl)phenol; IT1t, (*Z*)-6,6-dimethyl-5,6-dihydroimidazo[2,1-*b*]thiazole-3-yl-*N*,*N*′-dicycylohexylcarbamimidothioate; ML056, (*R*)-3-amino-(3-hexylphenylamino)-4-oxobutylphosphonic acid; CVX15, cyclic disulfide of H-Arg-Arg-Nal-Cys-Tye-Gln-Lys-D-Pro-Pro-Tyr-Arg-Cit-Cys-Arg-Gly-D-Pro-OH.

TABLE 1

Crystal structures of GPCRs deposited in the Protein Data Bank (www.rcsb.org) at the time of this writing

A total of 73 structures for 15 distinct receptors have been published: 20 for bovine rhodopsin, 4 for squid rhodopsin, 12 for the $\beta_1$-adrenergic receptor, 11 for the $\beta_2$-adrenergic receptor, 11 for the $A_{2A}$ adenosine receptor, 5 for the CXCR4 chemokine receptor, 1 for the $D_3$ dopamine receptor, 1 for the $H_1$ histamine receptor, 1 for the $M_2$ muscarinic acetylcholine receptor, 1 for the $M_3$ muscarinic receptor, 2 for the $S1P_1$ receptor, 1 for the κ-opioid receptor, 1 for the μ-opioid receptor, 1 for the δ-opioid receptor, and 1 for the nociceptin/orphanin FQ (NOP) receptor.

| Receptor and PDB ID | Ligand | Putative State | Res. | Reference |
|---|---|---|---|---|
| | | | Å | |
| Bovine rhodopsin | | | | |
| 1F88 | 11-*cis*-Retinal | Ground state | 2.80 | Palczewski et al., 2000 |
| 1HZX | 11-*cis*-Retinal | Ground state | 2.80 | Teller et al., 2001 |
| 1L9H | 11-*cis*-Retinal | Ground state | 2.60 | Okada et al., 2002 |
| 1U19 | 11-*cis*-Retinal | Ground state | 2.20 | Okada et al., 2004 |
| 1GZM | 11-*cis*-Retinal | Ground state | 2.65 | Li et al., 2004 |
| 2G87 | all-*trans*-Retinal (distorted) | Bathorhodopsin | 2.60 | Nakamichi and Okada, 2006a |
| 2HPY | all-*trans*-Retinal | Lumirhodopsin | 2.80 | Nakamichi and Okada, 2006b |
| 2I35 | 11-*cis*-retinal | Ground state | 3.80 | Salom et al., 2006 |
| 2I36 | 11-*cis*-retinal | Ground state | 4.10 | Salom et al., 2006 |
| 2I37[a,b] | all-*trans* Retinal | Early photoactivation | 4.15 | Salom et al., 2006 |
| 2PED | 9-*cis*-Retinal | Intermediate | 3.40 | Nakamichi et al., 2007 |
| 2J4Y[c] | 11-*cis*-Retinal | Isorhodopsin | 2.65 | Standfuss et al., 2007 |
| 3C9L[d] | 11-*cis*-Retinal | Ground state | 3.40 | Stenkamp, 2008 |
| 3C9M[e] | 11-*cis*-Retinal | Ground state | 2.60 | Stenkamp, 2008 |
| 3CAP[b] | Unliganded | Ground state | 2.90 | Park et al., 2008 |
| 3DQB[f] | Unliganded | Activated opsin | 2.70 | Scheerer et al., 2008 |
| 3OAX | 11-*cis*-Retinal and β-ionone | Activated opsin | 2.95 | Makino et al., 2010 |
| 2X72[f,g] | all-*trans* Retinal | Ground state | 3.00 | Standfuss et al., 2011 |
| 3PQR[f] | all-*trans* Retinal | Metarhodopsin II | 2.85 | Choe et al., 2011 |
| 3PXO | all-*trans* Retinal | Metarhodopsin II | 3.00 | Choe et al., 2011 |
| | | Metarhodopsin II | | |
| Squid rhodopsin | | | | |
| 2ZIY | 11-*cis*-Retinal | Ground state | 3.70 | Shimamura et al., 2008 |
| 2Z73 | 11-*cis*-Retinal | Ground state | 2.50 | Murakami and Kouyama, 2008 |
| 3AYM | all-*trans*-Retinal | Bathorhodopsin | 2.80 | Murakami and Kouyama, 2011 |
| 3AYN | 9-*cis*-Retinal | Isorhodopsin | 2.70 | Murakami and Kouyama, 2011 |
| Turkey $\beta_1$ adrenergic receptor | | | | |
| 2VT4[c] | Cyanopindolol (antagonist) | Inactive | 2.70 | Warne et al., 2008 |
| 2Y00[c] | Dobutamine (partial agonist) | Inactive | 2.50 | Warne et al., 2011 |
| 2Y01[c] | Dobutamine (partial agonist) | Inactive | 2.60 | Warne et al., 2011 |
| 2Y02[c] | Carmoterol (full agonist) | Inactive | 2.60 | Warne et al., 2011 |
| 2Y03[c] | Isoprenaline (full agonist) | Inactive | 2.85 | Warne et al., 2011 |
| 2Y04[c] | Salbutamol (partial agonist) | Inactive | 3.05 | Warne et al., 2011 |
| 2YCW[c,h] | Carazolol (antagonist) | Inactive | 3.00 | Moukhametzianov et al., 2011 |
| 2YCX[c,h] | Cyanopindolol (antagonist) | Inactive | 3.25 | Moukhametzianov et al., 2011 |
| 2YCY[c] | Cyanopindolol (antagonist) | Inactive | 3.15 | Moukhametzianov et al., 2011 |
| 2YCZ[c] | Iodocyanopindolol (antagonist) | Inactive | 3.65 | Moukhametzianov et al., 2011 |
| 4AMI[c] | Bucindolol (biased agonist) | Inactive | 3.20 | Warne et al., 2012 |
| 4AMJ[c] | Carvedilol (biased agonist) | Inactive | 2.30 | Warne et al., 2012 |
| Human $\beta_2$ adrenergic receptor | | | | |
| 2R4R[a,i] | Carazolol (inverse agonist)[j] | Inactive | 3.40 | Rasmussen et al., 2007 |
| 2R4S[a,i] | Carazolol (inverse agonist)[j] | Inactive | 3.40 | Rasmussen et al., 2007 |
| 2RH1[b,k] | Carazolol (inverse agonist) | Inactive | 2.40 | Cherezov et al., 2007; Rosenbaum et al., 2007 |
| 3D4S[k] | Timolol (inverse agonist) | Inactive | 2.80 | Hanson et al., 2008 |
| 3KJ6[a,i] | Carazolol (inverse agonist) | Inactive | 3.40 | Bokoch et al., 2010 |
| 3NY8[k] | ICI 118551 (inverse agonist) | Inactive | 2.84 | Wacker et al., 2010 |
| 3NY9[k] | Recent comp. (inverse-agonist) | Inactive | 2.84 | Wacker et al., 2010 |
| 3NYA[k] | Alprenolol (antagonist) | Inactive | 3.16 | Wacker et al., 2010 |
| 3PDS[k] | FAUC50 (irreversible agonist) | Inactive | 3.50 | Rosenbaum et al., 2011 |
| 3P0G[k,m] | BI-167107 (agonist) | Activated | 3.50 | Rasmussen et al., 2011a |
| 3SN6[k,m,j] | BI-167107 (agonist) | Activated | 3.20 | Rasmussen et al., 2011b |
| Human $A_{2A}$ adenosine receptor | | | | |
| 3EML[k] | ZM241385 (antagonist) | Inactive | 2.60 | Jaakola et al., 2008 |
| 2YDO[c] | Adenosine (agonist) | Inactive | 3.00 | Lebon et al., 2011 |
| 2YDV[c] | NECA (agonist) | Inactive | 2.60 | Lebon et al., 2011 |
| 3QAK[k] | UK-432097 | Activated | 2.71 | Xu et al., 2011 |
| 3PWH[c] | ZM241385 (antagonist) | Inactive | 3.30 | Doré et al., 2011 |
| 3REY[c] | XAC (antagonist) | Inactive | 3.31 | Doré et al., 2011 |
| 3RFM[c] | Caffeine (antagonist) | Inactive | 3.60 | Doré et al., 2011 |
| 3VG9[n] | ZM241385 (antagonist) | Inactive | 2.70 | Hino et al., 2012 |
| 3VGA[n] | ZM241385 (antagonist) | Inactive | 3.10 | Hino et al., 2012 |
| 3UZA[c] | 1,2,4-Triazine 4e (antagonist) | Inactive | 3.27 | Congreve et al., 2012 |
| 3UZC[c] | 1,2,4-Triazine 4g (antagonist) | Inactive | 3.24 | Congreve et al., 2012 |
| Human CXCR4 chemokine receptor | | | | |
| 3ODU[b,k] | IT1t (small mol. antagonists) | Inactive | 2.50 | Wu et al., 2010 |
| 3OE9[b,k] | IT1t (small mol. antagonists) | Inactive | 3.10 | Wu et al., 2010 |
| 3OE8[b,k] | IT1t (small mol. antagonists) | Inactive | 3.10 | Wu et al., 2010 |
| 3OE6[b,k] | IT1t (small mol. antagonists) | Inactive | 3.20 | Wu et al., 2010 |

TABLE 1—(*Continued*)

| Receptor and PDB ID | Ligand | Putative State | Res. | Reference |
|---|---|---|---|---|
| 3OE0[b,k] | CVX15 (peptide antagonist) | Inactive | 2.90 | Wu et al., 2010 |
| Human $D_3$ dopamine receptor | | | | |
| 3PBL[k] | Eticlopride (antagonist) | Inactive | 2.89 | Chien et al., 2010 |
| Human $H_1$ histamine receptor | | | | |
| 3RZE[k] | Doxepin (antagonist) | Inactive | 3.10 | Shimamura et al., 2011 |
| Human $M_2$ Muscarinic receptor | | | | |
| 3UON[k] | 3-Quinuclidinyl-benzilate (antagonist) | Inactive | 3.00 | Haga et al., 2012 |
| Rat $M_3$ Muscarinic receptor | | | | |
| 4DAJ[k] | Tiotropium (inverse agonist) | Inactive | 3.40 | Kruse et al., 2012 |
| Human $S1P_1$ sphingosine 1-phosphate receptor | | | | |
| 3V2Y[k,o] | ML056 (antagonist) | Inactive | 2.80 | Hanson et al., 2012 |
| 3V2W[k] | ML056 (antagonist) | Inactive | 3.35 | Hanson et al., 2012 |
| Human $\kappa$ opioid receptor | | | | |
| 4DJH[h,m] | JDTic (antagonist) | Inactive | 2.90 | Wu et al., 2012 |
| Mouse $\mu$ opioid receptor | | | | |
| 4DKL[b,k] | $\beta$-Funaltrexamine (irreversible antagonist) | Inactive | 2.80 | Manglik et al., 2012 |
| Mouse $\delta$ opioid receptor | | | | |
| 4EJ4[b,k] | Naltrindole (antagonist) | Inactive | 3.40 | Granier et al., 2012 |
| Human nociceptin/orphanin FQ (NOP) receptor | | | | |
| 4EA3[p] | Peptide mimetic c-24 (antagonist) | Inactive | 3.01 | Thompson et al., 2012 |

ICI 118551, *erythro-DL*-1-(7-methylindan-4-yloxy)-3-isopropylaminobutan-2-ol; BI-167107, 5-hydroxy-8-{2-[2-(2-methylphenyl)-1,1-dimethyl-ethylamino]-1-hydroxyethyl}-4*H*-benzo[1,4]oxazin-3-one; NECA, 5′-*N*-ethylcarboxamidoadenosine; XAC, xanthine amine congener; JDTic, (3*R*)-7-hydroxy-*N*-[(2*S*)-1-[(3*R*,4*R*)-4-(3-hydroxyphenyl)-3,4-dimethylpiperidin-1-yl]-3-methylbutan-2-yl]-1,2,3,4-tetrahydroisoquinoline-3-carboxamide.

[a] Ligand not visible.
[b] Potentially biologically relevant dimer observed in the structure.
[c] Thermally stable mutant receptor.
[d] Alternative model of 1GZM.
[e] Alternative model of 2J4Y.
[f] In complex with a C-terminal peptide of the $\alpha$-subunit of transducin.
[g] Constitutively active mutant.
[h] Showing an intact salt bridge linking the cytoplasmic ends of TMs 3 and 6.
[i] In complex with a fragment antigen-binding.
[j] In complex with a G protein ($G_s$) heterotrimer.
[k] T4-lysozyme fusion protein.
[l] (*R*)-5-(2-((4-(3-((2-Aminoethyl)disulfanyl)propoxy)-3-methoxyphenethyl)amino)-1-hydroxyethyl)-8-hyfroxyquinolin-2(1H)-one.
[m] In complex with a camelid antibody fragment.
[n] In complex with a fragment antigen-binding that prevents agonist binding.
[o] Processed with a microdiffraction data assembly method.
[p] Fusion protein with thermostabilized apocytochrome $b_{562}$RIL.

(Costanzi, 2012; Krishnan et al., 2012). As shown in Fig. 1, most of these receptors belong to a branch of class A that comprises receptors for biogenic amines melanocortin, endothelial differentiation sphingolipids, cannabinoid and adenosine receptors. The only exceptions are the chemokine CXCR4 and opioid receptors ($\kappa$ and $\mu$), which are found in a branch of class A predominantly populated by peptide receptors, and rhodopsin, which is found in a small branch of class A populated by opsins. Moreover, the solution of the nociceptin/orphanin FQ peptide receptor has recently been announced. A large portion of the dendrogram of class A GPCRs, including a branch that comprises mostly receptors for nucleotides and lipids, is still unexplored. There is reason to expect that many other structures will be solved in the near future to shed light onto a still-uncharted region of the GPCR phylogenetic dendrogram. Furthermore, the solution of receptors belonging to families beyond class A is expected.

The technical advances that led to this dramatic progress include the following:

1. Fusion of the receptor with the T4-lysozyme, which increases the tendency to form crystals—the T4-lysozyme is usually inserted in lieu of intracellular loop 3 (Cherezov et al., 2007; Rosenbaum et al., 2007) but has also been fused with the N terminus, to facilitate the cocrystallization of a receptor-G protein complex (Rasmussen et al., 2011b);
2. Structurally stabilizing point mutations, either in the ligand-binding regions or more remotely—this approach has been introduced by the groups in Cambridge and the associated company Heptares (Warne et al., 2008). These thermostabilizing mutations can be made to favor either an antagonist-bound conformation or agonist-bound conformation (although poorly activatable because of the energetic stabilization) of the same GPCR. The stabilization is so effective that the GPCR protein can be captured on a Biacore chip to allow characterization of small-molecule binding by measuring surface plasmon resonance (Zhukov et al., 2011);
3. Stabilization of the receptors through antibodies (Rasmussen et al., 2007)—recently, nanobodies generated in llamas inoculated with receptors as well as receptors cross-linked with G protein heterotrimers have been used to solve crystal structures of the activates state of the $\beta_2$-adrenergic receptor (Rasmussen et al., 2011a,b);
4. Specialized agonists, such as irreversibly binding agonists (Rosenbaum et al., 2011) or an agonist that has multiple arms extending from the core pharmacophore structure (Xu et al., 2011); and
5. Specialized techniques for producing crystals of membrane-bound proteins, including adaptation of the lipidic cubic phase, which forms a single lipid-aqueous bilayer that allows ordered protein molecules to make contacts in their hydrophobic as well as hydrophilic portions (Cherezov, 2011).

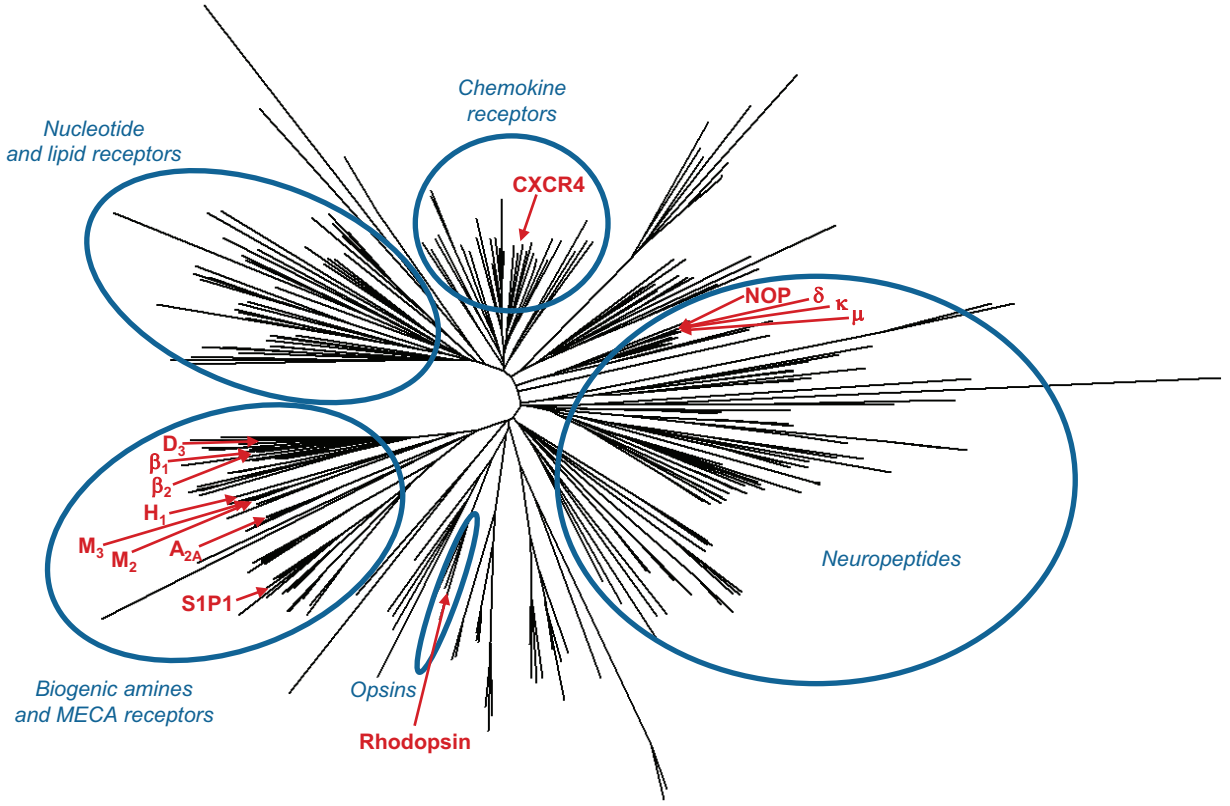


**Fig. 1.** Phylogenetic dendrogram of family A GPCRs based on aligned sequences. All the family members with solved crystal structures, except rhodopsin, the CXCR4 chemokine receptor, and the δ-, κ-, and μ-opioid receptors and the nociceptin/orphanin FQ (NOP) receptor, belong to a cluster of receptors for biogenic amines and MECA (melanocortin, endothelial differentiation sphingolipids, cannabinoid, and adenosine) receptors.

### The Ligand Binding Cavity

All GPCRs are constituted by a single polypeptide chain that spans the plasma membrane seven times with seven α-helical structures (Costanzi et al., 2009). As the crystal structures revealed, the helical bundle of most class A GPCRs hosts a ligand-binding cavity opened toward the extracellular milieu, which provides access to diffusible ligands. Alternately, the cavities of rhodopsin and $S1P_1$ receptor are sealed from the extracellular space by the second extracellular loop (EL2) and the N terminus, respectively. It is likely that the hydrophobic ligands of these receptors make their way into the binding cavity through the transmembrane domains. For most GPCRs, this ligand-binding cavity is lined by transmembrane domains (TMs) 2, 3, 5, 6, and 7 and is deeper in proximity to TMs 5 and

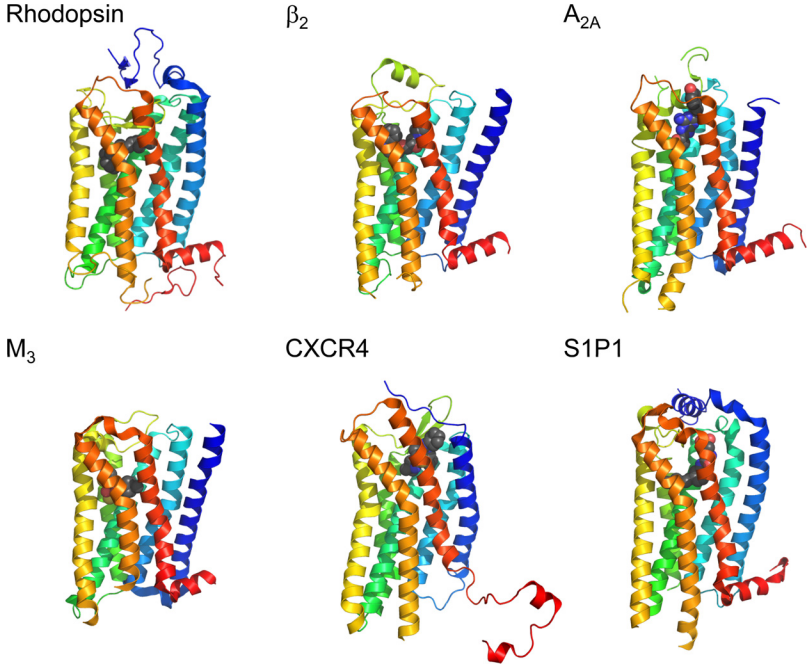


**Fig. 2.** Side-by-side comparison of the crystal structures of six representative receptors. All receptors show a common topology composed of seven transmembrane α helices connected by three extracellular and three intracellular loops. The N terminus is in the extracellular space, and the C terminus is in the cytosol. The cocrystallized ligands are found within an interhelical cavity open toward the extracellular milieu. The backbone of the receptors is represented schematically as a ribbon, with a color gradient ranging from blue at the N terminus to red at the C terminus (TM1, dark blue; TM2, pale blue; TM3, blue/green; TM4, green; TM5, yellow; TM6, yellow/orange; TM7, orange/red). The cocrystallized ligands are represented as van der Waals spheres, with the carbon atoms colored charcoal gray; oxygen atoms, red; nitrogen atoms, blue; and sulfur atoms, yellow.

6 but shallower in proximity to TMs 2 and 7 (Fig. 2). Nevertheless, in some cases, TMs 1 and 4 also form the pocket and can affect ligand binding. The various ligands cocrystallized with their receptors in the currently solved GPCR structures variously occupy different regions of this cavity. This is evident from Fig. 3, which shows a side-by-side comparison of six representative receptors featuring the bound ligands and the residues that surround them, as well as Fig. 4, which provides an overlay of the same ligands of these receptors resulting from a structural superposition of the receptors. It is noteworthy that different ligands that bind to the same receptor may occupy different regions of the binding cavity. This situation is particularly evident from Fig. 5A, which compares the binding, to the CXCR4 receptor, of a small molecule antagonist and a cyclic peptide antagonist (Wu et al., 2010): there is virtually no overlap between the two molecules. Less extreme is the case illustrated in Fig. 5B, which compares the binding to the adenosine receptor of a nonpurine antagonist and an adenosine-based agonist 2-(3-[1-(pyridin-2-yl)piperidin-4-yl]ureido)ethyl-6-*N*-(2,2-diphenylethyl)-5′-*N*-ethylcarboxamidoadenosine-2-carboxamide (UK-432097) bearing large substituents at the C2 and N6 positions of the purine ring (Xu et al., 2011): although there is substantial overlap between the two molecules, the larger agonist occupies regions of the receptor unexploited by the antagonist. The ribose moiety, which is an essential component of nearly all adenosine receptor agonists, confers to the ligand its agonistic properties. This moiety is accommodated in a space of the binding cavity close to TM3 that in the antagonist-bound state is unoccupied by a ligand and is partially filled by water molecules. The hydroxyl and other H-bonding groups of agonists displace these water molecules, thereby gaining an entropic advantage in the binding process. This is consistent with the typically nanomolar affinities of agonists at three of the four subtypes of adenosine receptors. The other large substituents present on the agonist UK-432097 cocrystallized with the $A_{2A}$

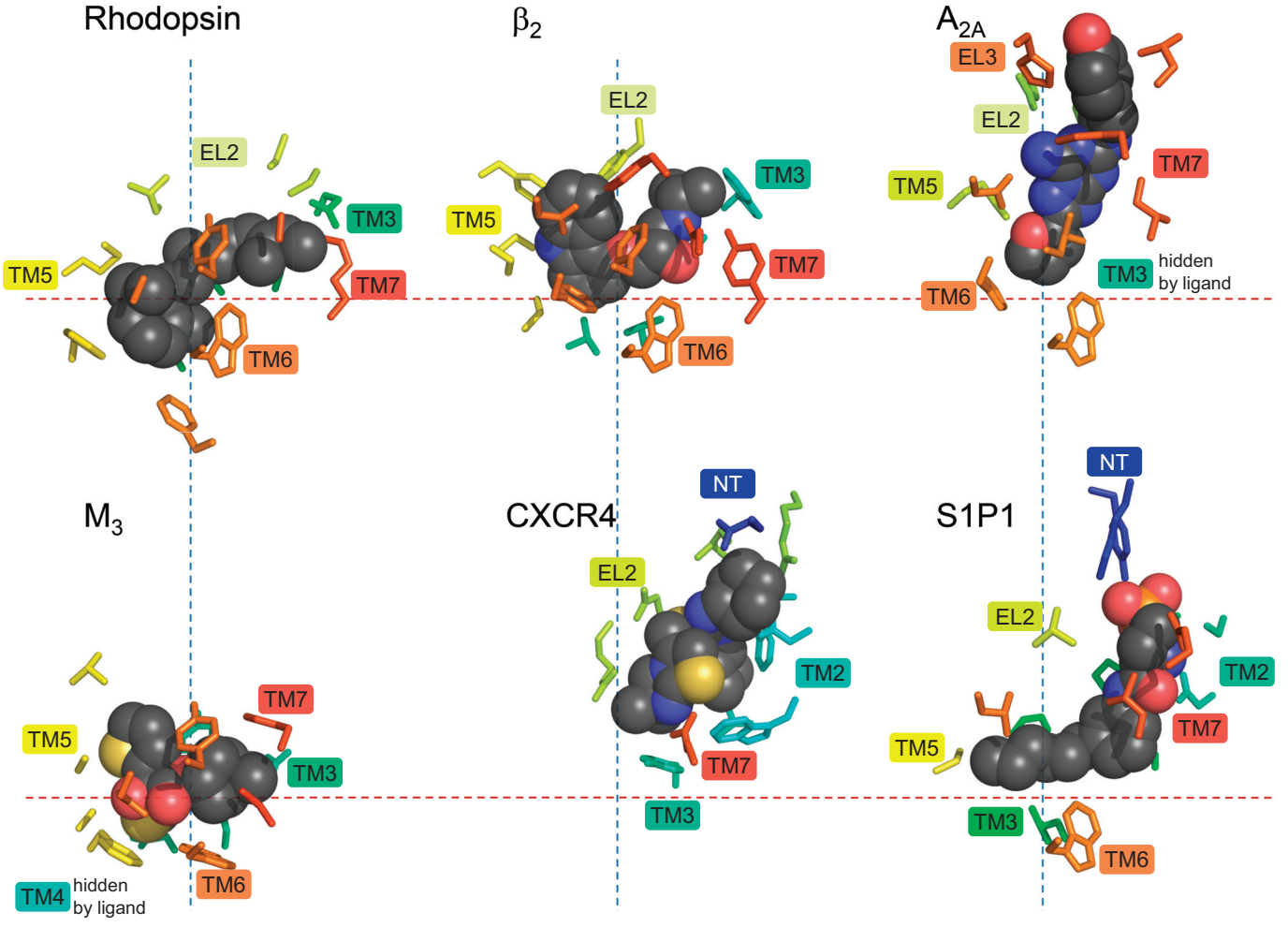


**Fig. 3.** The shown cocrystallized ligands—all antagonists or inverse agonists—are retinal for rhodopsin; carazolol [1-(9*H*-carbazol-4-yloxy)-3-(propan-2-ylamino)propan-2-ol] for the $\beta_2$-adrenergic receptor; ZM241385 for the $A_{2A}$ adenosine receptor; tiotropium [(1$\alpha$,2$\beta$,4$\beta$,7$\beta$)-7-[(hydroxidi-2-thienylacetyl)oxy]-9,9-dimethyl-3-oxa-9-azoniatricyclo[3.3.1.$0^{2,4}$]nonane bromide] for the muscarinic $M_3$ receptor; the small molecule antagonist IT1t [(*Z*)-6,6-dimethyl-5,6-dihydroimidazo[2,1-*b*]thiazole-3-yl-*N*,*N*′-dicycylohexylcarbamimidothioate] for the CXCR4 receptor; and ML056 [(*R*)-3-amino-(3-hexylphenylamino)-4-oxobutylphosphonic acid] for the $S1P_1$ receptor. Color-coded labels indicate the seven TMs, whereas, for selected residues, black labels indicate the GPCR residue index. The alignment of the six panels derives from a superposition of the receptors, which are oriented with their axes perpendicular to the plane of the membrane as in Fig. 2. To facilitate a comparison of the structural alignment of the binding cavities, dashed lines are drawn that intersect in correspondence to the conserved proline residue found in TM6 (Pro6.50 according to the GPCR residue indexing system). The red lines are parallel to the plane of the membrane, whereas the blue lines are perpendicular to it. As is evident, some ligands bind more deeply than others. Moreover, some ligands bind more toward TM5 (to the left of the blue line), and others bind more in the direction of TM2 (the right of the blue line).

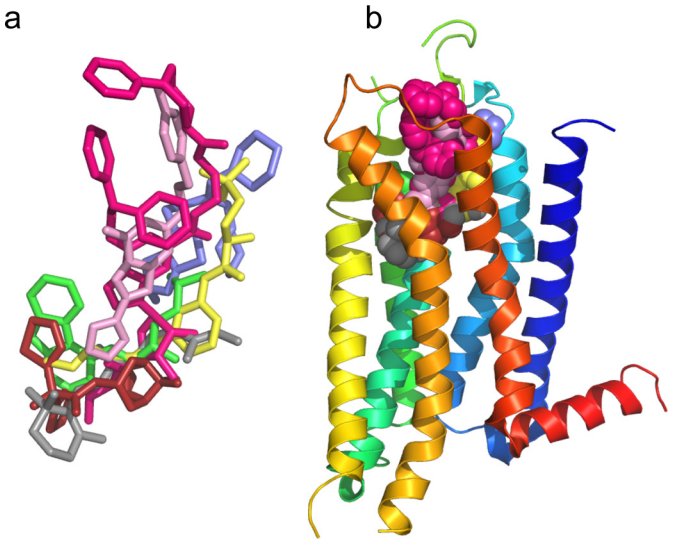


**Fig. 4.** a, an overlay of the six ligands of the six representative receptors shown in Figs. 1 and 2, resulting from a structural superposition of the receptors – retinal in gray, carazolol in green, ZM241385 in pink, tiotropium in dark red, IT1t in blue/purple, and ML056 in yellow. For the $A_{2A}$ adenosine receptor, the agonist UK-432097, in magenta, is also shown. b, the same ligands are shown within the backbone of the $A_{2A}$ receptor, represented schematically as a ribbon, with a color gradient ranging from blue at the N terminus to red at the C terminus (TM1, dark blue; TM2, pale blue; TM3, blue/green; TM4, green; TM5, yellow; TM6, yellow/orange; TM7, orange/red). The cocrystallized ligands are represented as van der Waals spheres, with the carbon atoms colored charcoal gray; oxygen atoms, red; nitrogen atoms, blue; and sulfur atoms, yellow.

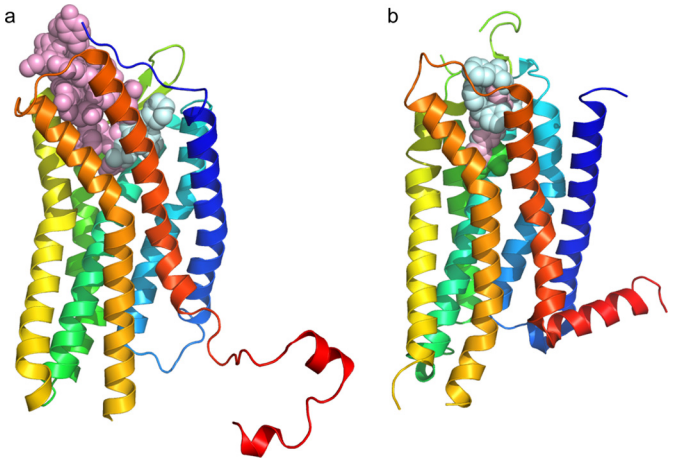


**Fig. 5.** Comparison of the binding mode of different ligands to the CXCR4 receptor (a) and the $A_{2A}$ adenosine receptor (b). In the case of the CXCR4 receptor, there is virtually no overlap between the bound small-molecule antagonist IT1t (pale blue) and the cyclic peptide antagonist CVX15 (cyclic disulfide of H-Arg-Arg-Nal-Cys-Tye-Gln-Lys-D-Pro-Pro-Tyr-Arg-Cit-Cys-Arg-Gly-D-Pro-OH; pale pink). In the case of the adenosine receptor, there is more commonality between the binding mode of the two ligands, but the larger agonist (pale blue) touches areas of the receptor that do not interact with the antagonist (pale pink). The ligands are represented as van der Waals spheres. The backbone of the receptors is represented schematically as a ribbon, with a color gradient ranging from blue at the N terminus to red at the C terminus (TM1, dark blue; TM2, pale blue; TM3, blue/green; TM4, green; TM5, yellow; TM6, yellow/orange; TM7, orange/red). The cocrystallized ligands are represented as van der Waals spheres, with the carbon atoms colored charcoal gray; oxygen atoms, red; nitrogen atoms, blue; and sulfur atoms, yellow.

receptor further enhance the binding affinity of the agonist by establishing contacts with the receptor.

The outer regions of a GPCR can serve as meta-binding sites for a ligand on its path to the principle orthosteric binding site and can also contribute to the lining of the orthosteric binding site. The X-ray structures have confirmed the hypothesis, based on mutagenesis as well as molecular modeling (Olah et al., 1994; Moro et al., 1999; Peeters et al., 2011), that parts of the ELs are intimately involved in recognition of ligands for both agonists and antagonists. In particular, we now know that the C-terminal part of EL2 tends to drop more or less deeply, depending on the receptor, into the ligand-binding region to establish contacts with the ligands (Fig. 3), as predicted using site-directed mutagenesis. Peculiar are the cases of rhodopsin and the $S1P_1$ receptor, in which the ligand-binding cavity is substantially more enclosed than in other receptors, thanks to a singular conformation of EL2 that occludes the entrance of the cleft (Palczewski et al., 2000). Conversely, the conformation that EL2 assumes in the chemokine CXCR4 receptor renders the binding cavity particularly open to the extracellular space, facilitating the binding of large peptides (Wu et al., 2010). However, the role of ELs in recognition of and activation by large peptide ligands will require further studies (Dong et al., 2011).

In general, the extracellular loops are typically more varied between subtypes than the TMs, which could facilitate the rational design of more selective orthosteric and allosteric ligands, as guided by the three-dimensional structures of the receptor complexes. For instance, the $M_2$ (Haga et al., 2012) and $M_3$ (Kruse et al., 2012) muscarinic acetylcholine receptors contain a vestibule in their outer portions that corresponds to the regions of the receptor associated with the binding of allosteric modulators. The fact that the orthosteric site of the muscarinic receptors and the specific residues involved in ligand recognition are identical across the family has impeded the medicinal chemical effort to design selective competitive ligands. The possibility of targeting the vestibule, which is more divergent in sequence, now offers further opportunities for drug design. However, for those receptors for which a crystallographically solved structure is not yet available, the high variability of the extracellular regions makes their modeling subject to greater uncertainty compared with the modeling of the seven TMs (Goldfeld et al., 2011).

**Inactive and Activated Structures.** The determination of both agonist- and antagonist-bound states of the same receptor was accomplished for two classes (i.e., $\beta$-adrenergic and adenosine receptors, in addition to visual pigment receptors with the structures of opsin and rhodopsin) (Park et al., 2008; Scheerer et al., 2008; Choe et al., 2011; Rasmussen et al., 2011a,b; Standfuss et al., 2011; Xu et al., 2011). This major step forward allowed a deeper understanding of the activation processes operating in GPCRs. Thus, the details of agonist binding and activation (i.e., characteristic agonist-induced movement of helices and key residues) are beginning to be understood. The comparison of the structures of inactive rhodopsin with those of the meta II state of rhodopsin as well as the unliganded opsin revealed several conformational changes associated with the activation of the receptor. The most notable of these conformational changes entail outward movements of the intracellular side of TM6 and movements of TM5 toward TM6 (Fig. 6, A and B). These conformational changes were also found in the agonist-bound $\beta_2$-adrenergic and $A_{2A}$ adenosine receptors, although the displacement of TM6 is substantially less pronounced in the $A_{2A}$ receptor because of the T4-lysozyme

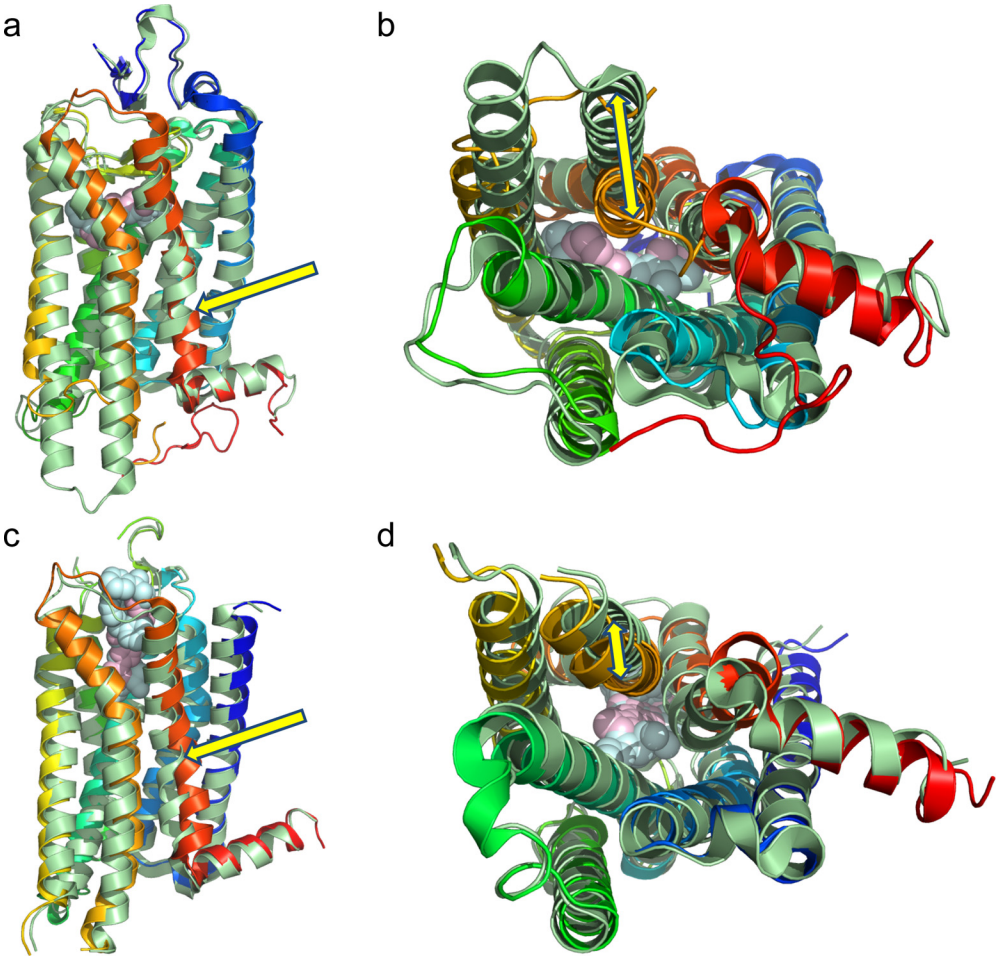


**Fig. 6.** Comparison of inactive and activated structures for rhodopsin (a and b) and for the $A_{2A}$ adenosine receptor (c and d). A seesaw movement of TM7 that is shifted toward the core of the receptor in the agonist bound structure is more evident in the $A_{2A}$ receptor than in rhodopsin (yellow arrows in a and c). Conversely, an outward movement of TM6 (yellow arrows in b and d, viewed from the cytosol) is more evident in rhodopsin than the adenosine $A_{2A}$ receptor, where the conformational change might have been hindered by the presence of a T4-lysozyme fused between TMs 5 and 6. The backbone of the inactive receptors is represented schematically, with a color gradient ranging from blue at the N terminus to red at the C terminus (TM1, dark blue; TM2, pale blue; TM3, blue/green; TM4, green; TM5, yellow; TM6, yellow/orange; TM7, orange/red). The ligands are represented as van der Waals spheres, with the agonists colored pale blue and the blockers colored pale pink.

fused between the cytosolic ends of TM5 and TM6 (Fig. 6, C and D). In addition, the distance between oppositely charged amino acid side chains near the cytosolic side (e.g., an Arg and an Asp residue, respectively, found in TMs 3 and 6 and predicted to be involved in a putative ionic lock characteristic of the inactive state, increased upon binding of the agonist in each case. However, it should be noted that this ionic lock was not fully closed in the inactive states of the $\beta_2$-adrenergic and $A_{2A}$ adenosine receptors. Furthermore, some movements that were not predicted in the opsin structure were seen in other receptors, such as a seesaw movement of TM7 in the $A_{2A}$ adenosine receptor by which the intracellular end moves inward (Fig. 5, C and D). Movements in the EL regions were also noted. These movements seem to be more ligand-specific than the movements in the TM regions. For example, the outward displacement of EL3 of the $A_{2A}$ adenosine receptor was considerably greater for an agonist having bulky substitutions of the adenine ring than in the unsubstituted cases. It is noteworthy that increasing evidence demonstrates that the stimulation of one GPCR can trigger different signaling cascades in a ligand-dependent manner through a phenomenon known as biased agonism (Kahsai et al., 2011). As a result, the same receptor can be selectively induced to activate a variety of pathways mediated by G proteins as well as $\beta$-arrestins. These different signaling states are probably due to distinct conformations of the same receptor that individual ligands can induce or stabilize. Further light will be shed on the correlation between conformation and signaling state of GPCRs once multiple structures of the same receptor with a variety of biased ligands are solved. In this respect, some progress has been made for the $\beta_1$- and $\beta_2$-adrenergic receptors through crystallographic (Warne et al., 2012) and NMR studies (Liu et al., 2012), respectively. For the $\beta_1$-adrenergic receptor, the crystal structures revealed that the biased agonists bucindolol and carvedilol, which stimulate $\beta$-arrestin-mediated signaling but act as inverse agonists or partial agonists of G protein-dependent pathways, interact with additional residues located in EL2 as well as TM7 compared with unbiased $\beta$-adrenergic receptor blockers. Moreover, the above-mentioned NMR spectroscopic analyses of the $\beta_2$-adrenergic receptor suggest that ligands, including biased ligands, do not "induce" states but shift equilibrium between pre-existing states. Specifically, the study indicates that unbiased ligands affect mostly the conformational state of TM6, whereas biased agonists shift primarily the conformational state of TM7 (Liu et al., 2012).

## Molecular Docking at GPCR Homology Models to Predict the Structure of Receptor Ligand Complexes

Until recently, the three-dimensional study of the interactions of GPCRs with their ligands was limited to molecular modeling. The modeling efforts began more than 2 decades ago, using as a crude template the structure of bacteriorhodopsin, and progressed with the major advance of the high-resolution structure of bovine rhodopsin more than a decade ago (Ballesteros et al., 2001; Costanzi et al., 2007, 2009). Although there has been much variability in the confidence in the modeling results (articles were published with diamet-

rically opposed modes of ligand binding for the same receptor-ligand complex), there were examples of well supported modeling that was later validated crystallographically (among others, see Ivanov et al., 2009; Michino et al., 2009; Kufareva et al., 2011). Comparisons of crystal structures and homology models revealed that, for some GPCRs, reasonably accurate receptor-ligand complexes can be constructed through homology modeling followed by molecular docking (Costanzi, 2008, 2010, 2012; Reynolds et al., 2009). However, accurate complexes cannot always be obtained through the sole use of specialized software. Purely computational docking of ligands at GPCR homology models could lead to substantially inaccurate results if the contributions of specific residues to ligand biding or, even worse, the location of the binding cavity were incorrectly recognized. A community-wide challenge to molecular modelers to predict the docking mode of antagonist 4-(2-(7-amino-2-(furan-2-yl)-[1,2,4]triazolo[1,5-*a*][1,3,5]triazin-5-ylamino)ethyl)phenol (ZM241385) to the $A_{2A}$ adenosine receptor before the release of the X-ray structure showed how the ligand could assume almost a random placement around the receptor (Michino et al., 2009). However, when informed with accessory information about the molecular recognition elements, the placement of the ligand in various docking models was shown to be within a reasonable range of accuracy (Michino et al., 2009). In many cases, the identification of the correct receptor-ligand interactions is strictly dependent on an expert selection of the docking poses based on insights derived from site-directed mutagenesis, comparisons of SAR within the same chemical series, and bioinformatics studies within a receptor family.

A further controlled assessment clarified that, when the target receptor shares a significant sequence similarity with one of the available templates, the models are particularly accurate. Conversely, predictions are more challenging for receptors that are more distant from the available templates, in which case the modeling strategies need to be more closely guided through the incorporation of the above-mentioned external information (Kufareva et al., 2011). Because, as we pointed out, there are not yet X-ray structures representative of all major branches of the GPCR dendrogram (Fig. 1), the modeling of receptors that are more distant from the available templates is still challenging. Moreover, the modeling of GPCRs belonging to classes B and C (Hu et al., 2006; Wheatley et al., 2012) remains more uncertain, because none of the structures of the members of these families have been solved crystallographically.

As mentioned, particularly important is the use of data gathered from site-directed mutagenesis. In this regard, one variation of the use of site-directed mutagenesis that has been particularly informative with respect to probing molecular recognition among GPCRs has been that of re-engineering the binding site to accept agonists that have been chemically modified. These approaches, with some important differences, are known by various terms introduced by different research groups: neoceptors, "receptors activated solely by synthetic ligands," and "designer receptors exclusively activated by designer drugs" (Conklin et al., 2008). Different degrees of design insight versus empirical screening have been used to match a given mutant receptor with an orthogonally activating agonist analog. The neoceptor approach, in particular, has focused on the adenosine receptor family to accurately predict the placement of the ribose moiety of nucleoside agonists, using the three-way integrated combination of mutagenesis, modeling, and chemical modification. Complementary changes in the structures of the ligand and receptor that lead to enhanced affinity can help establish the orientation of a ligand within the binding site.

Receptor-ligand interactions can also be studied through a systematic approach that was recently introduced, termed biophysical mapping (Zhukov et al., 2011). This method is based on the characterization of the functional contour of the binding pocket of a given GPCR using a thermostabilized form of the receptor. The effects of site-directed mutagenesis within the binding site are correlated with binding data for diverse ligands obtained through SPR measurements. Then, molecular modeling and docking are used to map the small molecule-binding site with respect to each chemical class of ligands. This approach was used to identify novel chemotypes (later to be optimized by chemical modification), such as chromones and triazines, binding to the $A_{2A}$ adenosine receptor (Congreve et al., 2012; Langmead et al., 2012).

### Structure-Based Discovery of GPCR Ligands Is Increasingly More Practical

Looking ahead, it will be increasingly feasible to tap the potential of structure-based design for GPCRs, initially for class A (Congreve et al., 2011; Salon et al., 2011), and then, hopefully, for the other classes as well. For now, the newly revealed detailed knowledge of GPCR structures has already facilitated a recent flurry of studies directed toward ligand discovery.

The careful stepwise modification of known classes of agonist or antagonist for a given receptor has been for years a major successful approach of medicinal chemists when applied empirically. This study can now be expedited using accurate three-dimensional knowledge of receptor-ligand recognition. For instance, it is now feasible to target specific amino acid residues near the bound pharmacophore that might confer enhanced affinity or receptor subtype selectivity to the modified ligands. For example, recent reports have shown that $A_{2A}$ adenosine receptor agonists and antagonists can be modified in this manner (Congreve et al., 2012; Deflorian et al., 2012). Moreover, the interaction of small fragments with regions of the binding cavity proximal to the ligand, to be considered as candidate substituents to enhance the receptor-ligand interactions, can also be studied. In this context, in recent studies, the structure of a known GPCR agonist was systematically varied using the ICM software (Internal Coordinate Mechanics; Molsoft LLC, San Diego, CA). A library of 2000 small fragments was screened in silico for fit within a small pocket, to successfully predict those favoring adenosine receptor affinity when linked to the 5′-carbonyl group of modified adenosine (Tosh et al., 2012).

For the identification of ligands based on novel chemotypes, a technique that has proven its value is the virtual screening through molecular docking of chemically diverse libraries for the discovery of novel chemotypes that bind to various GPCRs (Costanzi, 2011). A number of controlled experiments targeting the $\beta$-adrenergic and adenosine receptors, conducted by subjecting to molecular docking known agonists and blockers together with a larger number of non-binders, clearly illustrated that such virtual screening campaigns are most effective when applied to X-ray structures (Reynolds et al., 2009; Vilar et al., 2010, 2011a; Costanzi and

Vilar, 2012). This observation is consistent with the successful identification of novel structurally diverse ligands on the basis of virtual screenings conducted by targeting the crystal structures of β-adrenergic, adenosine, dopamine, and histamine receptors (Sabio et al., 2008; Kolb et al., 2009; Carlsson et al., 2010, 2011; Katritch et al., 2010a; de Graaf et al., 2011; van der Horst et al., 2011; Langmead et al., 2012). The above-mentioned controlled experiments also demonstrated that virtual screening campaigns, although not as effective as when applied to a crystal structure, are useful when applied to accurate homology models (Cavasotto et al., 2008; Katritch et al., 2010b; Phatak et al., 2010; Vilar et al., 2010, 2011a; Cavasotto, 2011). This observation is in line with the results of virtual screening campaigns through which, before the explosion of GPCR crystallography, novel GPCR ligands were identified using rhodopsin-based homology models (Engel et al., 2008; Tikhonova et al., 2008). More recently, Carlsson et al. (2011) conducted a virtual screening campaign by targeting the crystal structure of the dopamine $D_3$ receptor as well as a model of the same receptor based on the $\beta_2$-adrenergic homolog, with which it shares a relatively high sequence identity (38% within the TMs and 61% within the binding cavity, defined as the residues found within a 4 Å radius from the bound ligands). It is noteworthy that each of these two parallel campaigns yielded two overlapping sets of novel ligands, suggesting that models based on a relatively close template are indeed useful to ligand discovery.

Controlled experiments demonstrated also that not only blockers but also agonists are substantially prioritized over nonbinders in docking experiments (Costanzi and Vilar, 2012). In particular, such controlled virtual screening campaigns revealed that the activated structure of the $\beta_2$-adrenergic receptor is significantly biased toward the preferential recognition of agonists over blockers. Moreover, they also showed that structures of receptors crystallized in the inactive state can be modified in silico by modeling the shape of the binding cavity around a docked agonist, thus being turned into structures that preferentially recognize agonists rather than blockers (Vilar et al., 2011b; Costanzi and Vilar, 2012). However, the identification of agonists on the basis of novel chemotypes through the screening of diverse libraries may prove particularly challenging, in light of the likely stricter structural requirements for agonism than for blockade. Moreover, as mentioned, it is increasingly evident that the same GPCR may trigger a variety of different signaling cascades (Kahsai et al., 2011). The basis for distinguishing ligands needed for selective effector pathway activation (i.e., biased ligands) is an important area for future investigation. Several examples of ligand-specific interactions of the same receptor have been reported, but the implications of these differences for signaling are still largely unknown.

Undoubtedly, docking-based virtual screening campaigns will become increasingly more feasible with the experimental determination of new GPCR structures. Moreover, they will also benefit from the fast pace at which supercomputing is progressing as well as the continuous improvement of computational algorithms. In particular, the scoring functions that are currently used to estimate the likelihood of binding of large sets of screened compounds represent a compromise between accuracy and rapidity. Large computer clusters as well as specialized purpose-built supercomputers will increasingly allow the development and application of more complex methods for the calculation of free binding energies (Mitchell and Matsumoto, 2011). Moreover, an increasingly higher number of alternative receptor conformations, either solved experimentally or generated computationally from a single experimental structure, will be applicable in parallel to the screening campaigns. This practice, known as receptor-ensemble docking, was already demonstrated to significantly improve virtual screening yields by providing a means to account for receptor flexibility (Bottegoni et al., 2011; Costanzi, 2011; Vilar et al., 2011a; Costanzi and Vilar, 2012).

## Conclusions

On the basis of methodological advances in X-ray crystallography, the structural elucidation of GPCRs has begun a revolution in the medicinal chemical approaches applied to the discovery of new GPCR ligands. The binding sites of different receptors partly overlap but differ significantly in ligand orientation, depth and breadth of contact areas in TM regions, and the involvement of the ELs. Conformational changes associated with activation have been analyzed for several receptors. However, there are still large areas in which knowledge is lacking. For example, there still is an uncharacterized large portion of the GPCR phylogenetic dendrogram, the interaction of large peptide ligands with their receptors are unclear, and the structural basis for functional selectivity (i.e., why agonists display different spectra of activation properties through the same GPCR) are poorly understood. Molecular modeling, informed by supporting information from site-directed mutagenesis and structure activity relationships, has been validated as a useful tool to extend structural insights to related GPCRs and to analyze docking of other ligands in already crystallized GPCRs. Further exploration of the interactions of GPCRs with their G protein and non–G-protein intracellular targets, through medicinal chemistry as well as techniques of structural biology, will undoubtedly be required.

### Authorship Contributions

*Wrote or contributed to the writing of the manuscript:* Jacobson and Costanzi.

### References


Ballesteros JA, Shi L, and Javitch JA (2001) Structural mimicry in G protein-coupled receptors: implications of the high-resolution structure of rhodopsin for structure-function analysis of rhodopsin-like receptors. *Mol Pharmacol* **60:**1–19.

Bokoch MP, Zou Y, Rasmussen SG, Liu CW, Nygaard R, Rosenbaum DM, Fung JJ, Choi HJ, Thian FS, Kobilka TS, et al. (2010) Ligand-specific regulation of the extracellular surface of a G-protein-coupled receptor. *Nature* **463:**108–112.

Bottegoni G, Rocchia W, Rueda M, Abagyan R, and Cavalli A (2011) A Systematic exploitation of multiple receptor conformations for virtual ligand screening. *PLoS One* **6:**e18845.

Carlsson J, Coleman RG, Setola V, Irwin JJ, Fan H, Schlessinger A, Sali A, Roth BL, and Shoichet BK (2011) Ligand discovery from a dopamine $D_3$ receptor homology model and crystal structure. *Nat Chem Biol* **7:**769–778.

Carlsson J, Yoo L, Gao ZG, Irwin JJ, Shoichet BK, and Jacobson KA (2010) Structure-based discovery of $A_{2A}$ adenosine receptor ligands. *J Med Chem* **53:**3748–3755.

Cavasotto CN (2011) Homology models in docking and high-throughput docking. *Curr Top Med Chem* **11:**1528–1534.

Cavasotto CN, Orry AJ, Murgolo NJ, Czarniecki MF, Kocsi SA, Hawes BE, O'Neill KA, Hine H, Burton MS, Voigt JH, et al. (2008) Discovery of novel chemotypes to a G-protein-coupled receptor through ligand-steered homology modeling and structure-based virtual screening. *J Med Chem* **51:**581–588.

Cherezov V (2011) Lipidic cubic phase technologies for membrane protein structural studies. *Curr Opin Struct Biol* **21:**559–566.

Cherezov V, Rosenbaum DM, Hanson MA, Rasmussen SG, Thian FS, Kobilka TS, Choi HJ, Kuhn P, Weis WI, Kobilka BK, et al. (2007) High-resolution crystal structure of an engineered human β2 adrenergic G protein-coupled receptor. *Science* **318:**1258–1265.

Chien EY, Liu W, Zhao Q, Katritch V, Han GW, Hanson MA, Shi L, Newman AH,

Javitch JA, Cherezov V, et al. (2010) Structure of the human dopamine $D_3$ receptor in complex with a D2/D3 selective antagonist. *Science* **330:**1091–1095.
Choe HW, Kim YJ, Park JH, Morizumi T, Pai EF, Krauss N, Hofmann KP, Scheerer P, and Ernst OP (2011) Crystal structure of metarhodopsin II. *Nature* **471:**651–655.
Congreve M, Andrews SP, Doré AS, Hollenstein K, Hurrell E, Langmead CJ, Mason JS, Ng IW, Tehan B, Zhukov A, et al. (2012) Discovery of 1,2,4-Triazine Derivatives as Adenosine $A_{2A}$ Antagonists using Structure Based Drug Design. *J Med Chem* **55:**1898–1903.
Congreve M, Langmead CJ, Mason JS, and Marshall FH (2011) Progress in Structure Based Drug Design for G Protein-Coupled Receptors. *J Med Chem* **54:**4283–4311.
Conklin BR, Hsiao EC, Claeysen S, Dumuis A, Srinivasan S, Forsayeth JR, Guettier JM, Chang WC, Pei Y, McCarthy KD, et al. (2008) Engineering GPCR signaling pathways with RASSLs. *Nat Methods* **5:**673–678.
Costanzi S (2008) On the applicability of GPCR homology models to computer-aided drug discovery: a comparison between in silico and crystal structures of the $\beta_2$ adrenergic receptor. *J Med Chem* **51:**2907–2914.
Costanzi S (2010) Modelling G protein-coupled receptors: a concrete possibility. *Chim Oggi* **28:**26–30.
Costanzi S (2011) Structure-based virtual screening for ligands of G protein-coupled receptors, in *G Protein-Coupled Receptors: From Structure to Function* (Giraldo J and Pin JP eds) pp 359–374, The Royal Society of Chemistry, London, UK.
Costanzi S (2012) Homology modeling of class a G protein-coupled receptors. *Methods Mol Biol* **857:**259–279.
Costanzi S, Ivanov A, Tikhonova I, and Jacobson K (2007) Structure and function of G protein-coupled receptors studied through using sequence analysis, molecular modeling and receptor engineering: adenosine receptors, in *Frontiers in Drug Design and Discovery* (Atta-ur-Rahman, Caldwell GW, Choudhary MI, Player MR, eds) pp 63–69, Bentham, Bussum, The Netherlands.
Costanzi S, Siegel J, Tikhonova IG, and Jacobson KA (2009) Rhodopsin and the others: a historical perspective on structural studies of G protein-coupled receptors. *Curr Pharm Des* **15:**3994–4002.
Costanzi S and Vilar S (2012) In silico screening for agonists and blockers of the $\beta_2$ adrenergic receptor: Implications of inactive and activated state structures. *J Comput Chem* **33:**561–572.
de Graaf C, Kooistra AJ, Vischer HF, Katritch V, Kuijer M, Shiroishi M, Iwata S, Shimamura T, Stevens RC, de Esch IJ, et al. (2011) Crystal structure-based virtual screening for fragment-like ligands of the human histamine $H_1$ receptor. *J Med Chem* **54:**8195–8206.
Deflorian F, Kumar TS, Phan K, Gao ZG, Xu F, Wu H, Katritch V, Stevens RC, and Jacobson KA (2012) Evaluation of molecular modeling of agonist binding in light of the crystallographic structure of an agonist-bound $A_{2A}$ adenosine receptor. *J Med Chem* **55:**538–552.
Dong M, Lam PC, Pinon DI, Hosohata K, Orry A, Sexton PM, Abagyan R, and Miller LJ (2011) Molecular basis of secretin docking to its intact receptor using multiple photolabile probes distributed throughout the pharmacophore. *J Biol Chem* **286:**23888–23899.
Doré AS, Robertson N, Errey JC, Ng I, Hollenstein K, Tehan B, Hurrell E, Bennett K, Congreve M, Magnani F, et al. (2011) Structure of the adenosine $A_{2a}$ receptor in complex with ZM241385 and the xanthines XAC and caffeine. *Structure* **19:**1283–1293.
Engel S, Skoumbourdis AP, Childress J, Neumann S, Deschamps JR, Thomas CJ, Colson AO, Costanzi S, and Gershengorn MC (2008) A virtual screen for diverse ligands: discovery of selective G protein-coupled receptor antagonists. *J Am Chem Soc* **130:**5115–5123.
Goldfeld DA, Zhu K, Beuming T, and Friesner RA (2011) Successful prediction of the intra- and extracellular loops of four G-protein-coupled receptors. *Proc Natl Acad Sci USA* **108:**8275–8280.
Granier S, Manglik A, Kruse AC, Kobilka TS, Thian FS, Weis WI, and Kobilka BK (2012) Structure of the δ-opioid receptor bound to naltrindole. *Nature* **485:**400–404.
Haga K, Kruse AC, Asada H, Yurugi-Kobayashi T, Shiroishi M, Zhang C, Weis WI, Okada T, Kobilka BK, Haga T, et al. (2012) Structure of the human M2 muscarinic acetylcholine receptor bound to an antagonist. *Nature* **482:**547–551.
Hanson MA, Cherezov V, Griffith MT, Roth CB, Jaakola VP, Chien EY, Velasquez J, Kuhn P, and Stevens RC (2008) A specific cholesterol binding site is established by the 2.8 Å structure of the human $\beta_2$ adrenergic receptor. *Structure* **16:**897–905.
Hanson MA, Roth CB, Jo E, Griffith MT, Scott FL, Reinhart G, Desale H, Clemons B, Cahalan SM, Schuerer SC, et al. (2012) Crystal structure of a lipid G protein-coupled receptor. *Science* **335:**851–855.
Hino T, Arakawa T, Iwanari H, Yurugi-Kobayashi T, Ikeda-Suno C, Nakada-Nakura Y, Kusano-Arai O, Weyand S, Shimamura T, Nomura N, et al. (2012) G-protein-coupled receptor inactivation by an allosteric inverse-agonist antibody. *Nature* **482:**237–240.
Hu J, Jiang J, Costanzi S, Thomas C, Yang W, Feyen JH, Jacobson KA, and Spiegel AM (2006) A missense mutation in the seven-transmembrane domain of the human $Ca^{2+}$ receptor converts a negative allosteric modulator into a positive allosteric modulator. *J Biol Chem* **281:**21558–21565.
Ivanov AA, Barak D, and Jacobson KA (2009) Evaluation of homology modeling of G-protein-coupled receptors in light of the $A_{2A}$ adenosine receptor crystallographic structure. *J Med Chem* **52:**3284–3292.
Jaakola VP, Griffith MT, Hanson MA, Cherezov V, Chien EY, Lane JR, Ijzerman AP, and Stevens RC (2008) The 2.6 angstrom crystal structure of a human $A_{2A}$ adenosine receptor bound to an antagonist. *Science* **322:**1211–1217.
Kahsai AW, Xiao K, Rajagopal S, Ahn S, Shukla AK, Sun J, Oas TG, and Lefkowitz RJ (2011) Multiple ligand-specific conformations of the $\beta_2$ adrenergic receptor. *Nat Chem Biol* **7:**692–700.
Katritch V, Jaakola VP, Lane JR, Lin J, Ijzerman AP, Yeager M, Kufareva I, Stevens RC, and Abagyan R (2010a) Structure-based discovery of novel chemotypes for adenosine $A_{2A}$ receptor antagonists. *J Med Chem* **53:**1799–1809.
Katritch V, Rueda M, Lam PC, Yeager M, and Abagyan R (2010b) GPCR 3D homology models for ligand screening: lessons learned from blind predictions of adenosine $A_{2A}$ receptor complex. *Proteins* **78:**197–211.
Kolb P, Rosenbaum DM, Irwin JJ, Fung JJ, Kobilka BK, and Shoichet BK (2009) Structure-based discovery of $\beta_2$ adrenergic receptor ligands. *Proc Natl Acad Sci USA* **106:**6843–6848.
Krishnan A, Almén MS, Fredriksson R, and Schiöth HB (2012) The origin of GPCRs: identification of mammalian like Rhodopsin, Adhesion, Glutamate and Frizzled GPCRs in fungi. *PLoS One* **7:**e29817.
Kruse AC, Hu J, Pan AC, Arlow DH, Rosenbaum DM, Rosemond E, Green HF, Liu T, Chae PS, Dror RO, et al. (2012) Structure and dynamics of the M3 muscarinic acetylcholine receptor. *Nature* **482:**552–556.
Kufareva I, Rueda M, Katritch V, Stevens RC, Abagyan R, and GPCR Dock 2010 participants (2011) Status of GPCR modeling and docking as reflected by community-wide GPCR Dock 2010 assessment. *Structure* **19:**1108–1126.
Langmead CJ, Andrews SP, Congreve M, Errey JC, Hurrell E, Marshall FH, Mason JS, Richardson CM, Robertson N, Zhukov A, et al. (2012) Identification of novel adenosine $A_{2A}$ receptor antagonists by virtual screening. *J Med Chem* **55:**1904–1909.
Lebon G, Warne T, Edwards PC, Bennett K, Langmead CJ, Leslie AG, and Tate CG (2011) Agonist-bound adenosine $A_{2A}$ receptor structures reveal common features of GPCR activation. *Nature* **474:**521–555.
Li J, Edwards PC, Burghammer M, Villa C, and Schertler GF (2004) Structure of bovine rhodopsin in a trigonal crystal form. *J Mol Biol* **343:**1409–1438.
Liu JJ, Horst R, Katritch V, Stevens RC, and Wüthrich K (2012) Biased signaling pathways in $\beta_2$-adrenergic receptor characterized by $^{19}$F-NMR. *Science* **335:**1106–1110.
Makino CL, Riley CK, Looney J, Crouch RK, and Okada T (2010) Binding of more than one retinoid to visual opsins. *Biophys J* **99:**2366–2373.
Manglik A, Kruse AC, Kobilka TS, Thian FS, Mathiesen JM, Sunahara RK, Pardo L, Weis WI, Kobilka BK, and Granier S (2012) Crystal structure of the mu-opioid receptor bound to a morphinan antagonist. *Nature* **485:**321–326.
Michino M, Abola E, GPCR Dock 2008 participants, Brooks CL 3rd, Dixon JS, Moult J, and Stevens RC (2009) Community-wide assessment of GPCR structure modelling and ligand docking: GPCR Dock 2008. *Nat Rev Drug Discov* **8:**455–463.
Mitchell W and Matsumoto S (2011) Large-scale integrated super-computing platform for next generation virtual drug discovery. *Curr Opin Chem Biol* **15:**553–559.
Moro S, Hoffmann C, and Jacobson KA (1999) Role of the extracellular loops of G protein-coupled receptors in ligand recognition: a molecular modeling study of the human $P2Y_1$ receptor. *Biochemistry* **38:**3498–3507.
Moukhametzianov R, Warne T, Edwards PC, Serrano-Vega MJ, Leslie AG, Tate CG, and Schertler GF (2011) Two distinct conformations of helix 6 observed in antagonist-bound structures of a $\beta_1$ adrenergic receptor. *Proc Natl Acad Sci USA* **108:**8228–8232.
Murakami M and Kouyama T (2008) Crystal structure of squid rhodopsin. *Nature* **453:**363–367.
Murakami M and Kouyama T (2011) Crystallographic analysis of the primary photochemical reaction of squid rhodopsin. *J Mol Biol* **413:**615–627.
Nakamichi H, Buss V, and Okada T (2007) Photoisomerization mechanism of rhodopsin and 9-cis-rhodopsin revealed by x-ray crystallography. *Biophys J* **92:**L106–L108.
Nakamichi H and Okada T (2006a) Crystallographic analysis of primary visual photochemistry. *Angew Chem Int Ed Engl* **45:**4270–4273.
Nakamichi H and Okada T (2006b) Local peptide movement in the photoreaction intermediate of rhodopsin. *Proc Natl Acad Sci USA* **103:**12729–12734.
Okada T, Fujiyoshi Y, Silow M, Navarro J, Landau EM, and Shichida Y (2002) Functional role of internal water molecules in rhodopsin revealed by X-ray crystallography. *Proc Natl Acad Sci USA* **99:**5982–5987.
Okada T, Sugihara M, Bondar AN, Elstner M, Entel P, and Buss V (2004) The retinal conformation and its environment in rhodopsin in light of a new 2.2 A crystal structure. *J Mol Biol* **342:**571–583.
Olah ME, Jacobson KA, and Stiles GL (1994) Role of the second extracellular loop of adenosine receptors in agonist and antagonist binding. Analysis of chimeric $A_1/A_3$ adenosine receptors. *J Biol Chem* **269:**24692–24698.
Palczewski K, Kumasaka T, Hori T, Behnke CA, Motoshima H, Fox BA, Le Trong I, Teller DC, Okada T, Stenkamp RE, et al. (2000) Crystal structure of rhodopsin: A G protein-coupled receptor. *Science* **289:**739–745.
Park JH, Scheerer P, Hofmann KP, Choe HW, and Ernst OP (2008) Crystal structure of the ligand-free G-protein-coupled receptor opsin. *Nature* **454:**183–187.
Peeters MC, van Westen GJ, Li Q, and IJzerman AP (2011) Importance of the extracellular loops in G protein-coupled receptors for ligand recognition and receptor activation. *Trends Pharmacol Sci* **32:**35–42.
Phatak SS, Gatica EA, and Cavasotto CN (2010) Ligand-steered modeling and docking: a benchmarking study in class A G-protein-coupled receptors. *J Chem Inf Model* **50:**2119–2128.
Rasmussen SG, Choi HJ, Rosenbaum DM, Kobilka TS, Thian FS, Edwards PC, Burghammer M, Ratnala VR, Sanishvili R, Fischetti RF, et al. (2007) Crystal structure of the human $\beta_2$ adrenergic G-protein-coupled receptor. *Nature* **450:**383–387.
Rasmussen SG, Choi HJ, Fung JJ, Pardon E, Casarosa P, Chae PS, Devree BT, Rosenbaum DM, Thian FS, Kobilka TS, et al. (2011a) Structure of a nanobody-stabilized active state of the $\beta_2$ adrenoceptor. *Nature* **469:**175–180.
Rasmussen SG, DeVree BT, Zou Y, Kruse AC, Chung KY, Kobilka TS, Thian FS, Chae PS, Pardon E, Calinski D, et al. (2011b) Crystal structure of the $\beta_2$ adrenergic receptor-Gs protein complex. *Nature* **477:**549–555.
Reynolds KA, Katritch V, and Abagyan R (2009) Identifying conformational changes of the $\beta_2$ adrenoceptor that enable accurate prediction of ligand/receptor interactions and screening for GPCR modulators. *J Comput Aided Mol Des* **23:**273–288.

Rosenbaum DM, Cherezov V, Hanson MA, Rasmussen SG, Thian FS, Kobilka TS, Choi HJ, Yao XJ, Weis WI, Stevens RC, et al. (2007) GPCR engineering yields high-resolution structural insights into $\beta_2$ adrenergic receptor function. *Science* **318:**1266–1273.

Rosenbaum DM, Zhang C, Lyons JA, Holl R, Aragao D, Arlow DH, Rasmussen SG, Choi HJ, Devree BT, Sunahara RK, et al. (2011) Structure and function of an irreversible agonist-$\beta_2$ adrenoceptor complex. *Nature* **469:**236–240.

Sabio M, Jones K, and Topiol S (2008) Use of the X-ray structure of the $\beta_2$ adrenergic receptor for drug discovery. Part 2: Identification of active compounds. *Bioorg Med Chem Lett* **18:**5391–5395.

Salom D, Lodowski DT, Stenkamp RE, Le Trong I, Golczak M, Jastrzebska B, Harris T, Ballesteros JA, and Palczewski K (2006) Crystal structure of a photoactivated deprotonated intermediate of rhodopsin. *Proc Natl Acad Sci USA* **103:**16123–16128.

Salon JA, Lodowski DT, and Palczewski K (2011) The significance of G protein-coupled receptor crystallography for drug discovery. *Pharmacol Rev* **63:**901–937.

Scheerer P, Park JH, Hildebrand PW, Kim YJ, Krauss N, Choe HW, Hofmann KP, and Ernst OP (2008) Crystal structure of opsin in its G-protein-interacting conformation. *Nature* **455:**497–502.

Shimamura T, Hiraki K, Takahashi N, Hori T, Ago H, Masuda K, Takio K, Ishiguro M, and Miyano M (2008) Crystal structure of squid rhodopsin with intracellularly extended cytoplasmic region. *J Biol Chem* **283:**17753–17756.

Shimamura T, Shiroishi M, Weyand S, Tsujimoto H, Winter G, Katritch V, Abagyan R, Cherezov V, Liu W, Han GW, et al. (2011) Structure of the human histamine $H_1$ receptor complex with doxepin. *Nature* **475:**65–70.

Standfuss J, Edwards PC, D'Antona A, Fransen M, Xie G, Oprian DD, and Schertler GF (2011) The structural basis of agonist-induced activation in constitutively active rhodopsin. *Nature* **471:**656–660.

Standfuss J, Xie G, Edwards PC, Burghammer M, Oprian DD, and Schertler GF (2007) Crystal structure of a thermally stable rhodopsin mutant. *J Mol Biol* **372:**1179–1188.

Stenkamp RE (2008) Alternative models for two crystal structures of bovine rhodopsin. *Acta Crystallogr D Biol Crystallogr* **D64**:902–904.

Teller DC, Okada T, Behnke CA, Palczewski K, and Stenkamp RE (2001) Advances in determination of a high-resolution three-dimensional structure of rhodopsin, a model of G-protein-coupled receptors (GPCRs). *Biochemistry* **40:**7761–7772.

Tikhonova IG, Sum CS, Neumann S, Engel S, Raaka BM, Costanzi S, and Gershengorn MC (2008) Discovery of novel agonists and antagonists of the free fatty acid receptor 1 (FFAR1) using virtual screening. *J Med Chem* **51:**625–633.

Thompson AA, Liu W, Chun E, Katritch V, Wu H, Vardy E, Huang XP, Trapella C, Guerrini R, Calo G, et al. (2012) Structure of the nociceptin/orphanin FQ receptor in complex with a peptide mimetic. *Nature* **485:**395–399.

Tosh DK, Phan K, Gao ZG, Gakh AA, Xu F, Deflorian F, Abagyan R, Stevens RC, Jacobson KA, and Katritch V (2012) Optimization of adenosine 5′-carboxamide derivatives as adenosine receptor agonists using structure-based ligand design and fragment-based searching. *J Med Chem* **55:**4297–4308.

van der Horst E, van der Pijl R, Mulder-Krieger T, Bender A, and IJzerman AP (2011) Substructure-based virtual screening for adenosine $A_{2A}$ receptor ligands. *ChemMedChem* **6:**2302–2311.

Vilar S, Ferino G, Phatak SS, Berk B, Cavasotto CN, and Costanzi S (2011a) Docking-based virtual screening for ligands of G protein-coupled receptors: not only crystal structures but also in silico models. *J Mol Graph Model* **29:**614–623.

Vilar S, Karpiak J, Berk B, and Costanzi S (2011b) In silico analysis of the binding of agonists and blockers to the $\beta_2$ adrenergic receptor. *J Mol Graph Model* **29:**809–817.

Vilar S, Karpiak J, and Costanzi S (2010) Ligand and structure-based models for the prediction of ligand-receptor affinities and virtual screenings: development and application to the $\beta_2$ adrenergic receptor. *J Comput Chem* **31:**707–720.

Wacker D, Fenalti G, Brown MA, Katritch V, Abagyan R, Cherezov V, and Stevens RC (2010) Conserved binding mode of human $\beta_2$ adrenergic receptor inverse agonists and antagonist revealed by X-ray crystallography. *J Am Chem Soc* **132:**11443–11445.

Warne T, Edwards PC, Leslie AG, and Tate CG (2012) Crystal structures of a stabilized $\beta_1$ adrenoceptor bound to the biased agonists bucindolol and carvedilol. *Structure* **20:**841–849.

Warne T, Moukhametzianov R, Baker JG, Nehmé R, Edwards PC, Leslie AG, Schertler GF, and Tate CG (2011) The structural basis for agonist and partial agonist action on a $\beta_1$ adrenergic receptor. *Nature* **469:**241–244.

Warne T, Serrano-Vega MJ, Baker JG, Moukhametzianov R, Edwards PC, Henderson R, Leslie AG, Tate CG, and Schertler GF (2008) Structure of a $\beta_1$ adrenergic G-protein-coupled receptor. *Nature* **454:**486–491.

Wheatley M, Wootten D, Conner MT, Simms J, Kendrick R, Logan RT, Poyner DR, and Barwell J (2012) Lifting the lid on GPCRs: the role of extracellular loops. *Br J Pharmacol* **165:**1688–1703.

Wu B, Chien EY, Mol CD, Fenalti G, Liu W, Katritch V, Abagyan R, Brooun A, Wells P, Bi FC, et al. (2010) Structures of the CXCR4 chemokine GPCR with small-molecule and cyclic peptide antagonists. *Science* **330:**1066–1071.

Wu H, Wacker D, Mileni M, Katritch V, Han GW, Vardy E, Liu W, Thompson AA, Huang XP, Carroll FI, et al. (2012) Structure of the human kappa-opioid receptor in complex with JDTic. *Nature* **485:**327–332.

Xu F, Wu H, Katritch V, Han GW, Jacobson KA, Gao ZG, Cherezov V, and Stevens RC (2011) Structure of an Agonist-Bound Human $A_{2A}$ Adenosine Receptor. *Science* **332:**322–327.

Zhukov A, Andrews SP, Errey JC, Robertson N, Tehan B, Mason JS, Marshall FH, Weir M, and Congreve M (2011) Biophysical mapping of the adenosine $A_{2A}$ receptor. *J Med Chem* **54:**4312–4323.

**Address correspondence to:** Dr. Kenneth A. Jacobson, Laboratory of Bioorganic Chemistry, National Institutes of Diabetes and Digestive and Kidney Diseases, NIH, Bldg. 8A, Rm. B1A-19, Bethesda, MD 20892-0810. E-mail: kajacobs@helix.nih.gov